Natural and Anthropogenic Aerosol Trends from Satellite and Surface Observations and Model Simulations over the North Atlantic Ocean from 2002 to 2012

ANDREW R. JONGEWARD

Earth System Science Interdisciplinary Center, and Department of Atmospheric and Oceanic Science, University of Maryland, College Park, College Park, Maryland

ZHANQING LI

Earth System Science Interdisciplinary Center, and Department of Atmospheric and Oceanic Science, University of Maryland, College Park, College Park, Maryland, and State Key Laboratory of Earth Surface Processes and Resource Ecology, and College of Global Change and Earth System Science, Beijing Normal University, Beijing, China

HAO HE

Earth System Science Interdisciplinary Center, and Department of Atmospheric and Oceanic Science, University of Maryland, College Park, College Park, Maryland

XIAOXIONG XIONG

Biospheric Sciences Laboratory, NASA Goddard Space Flight Center, Greenbelt, Maryland

(Manuscript received 13 October 2015, in final form 21 June 2016)

ABSTRACT

Aerosols contribute to Earth's radiative budget both directly and indirectly, and large uncertainties remain in quantifying aerosol effects on climate. Variability in aerosol distribution and properties, as might result from changing emissions and transport processes, must be characterized. In this study, variations in aerosol loading across the eastern seaboard of the United States and the North Atlantic Ocean during 2002 to 2012 are analyzed to examine the impacts of anthropogenic emission control measures using monthly mean data from MODIS, AERONET, and IMPROVE observations and Goddard Chemistry Aerosol Radiation and Transport (GOCART) model simulation. MODIS observes a statistically significant negative trend in aerosol optical depth (AOD) over the midlatitudes (-0.030 decade^{-1}). Correlation analyses with surface AOD from AERONET sites in the upwind region combined with trend analysis from GOCART component AOD confirm that the observed decrease in the midlatitudes is chiefly associated with anthropogenic aerosols that exhibit significant negative trends from the eastern U.S. coast extending over the western North Atlantic. Additional analysis of IMPROVE surface $PM_{2.5}$ observations demonstrates statistically significant negative trends in the anthropogenic components with decreasing mass concentrations over the eastern United States. Finally, a seasonal analysis of observational datasets is performed. The negative trend seen by MODIS is strongest during spring (MAM) and summer (JJA) months. This is supported by AERONET seasonal trends and is identified from IMPROVE seasonal trends as resulting from ammonium sulfate decreases during these seasons.

1. Introduction

Aerosols contribute directly to atmospheric variability and to Earth's radiative balance through scattering and absorption of solar radiation. Aerosols also contribute indirectly through complex aerosol–cloud interactions (ACI). The Intergovernmental Panel on Climate Change (IPCC) Fifth Assessment Report (AR5) indicates that while the mechanisms of aerosol direct effects are well known, the uncertainties in the estimates of aerosol direct and indirect effects are larger than any other radiative forcing agent (IPCC 2013). Further in-depth studies are needed to probe and assess any long-term changes in aerosol and its ensuing changes in clouds and other climate variables.

Corresponding author address: Z. Li, GCESS and ESPRE, Beijing Normal University, Jingshi Science and Technology Bldg. B, College Road South, Haidian District, Beijing 100875, China.
E-mail: zhanqingli@msn.com

DOI: 10.1175/JAS-D-15-0308.1

Recent work has shown that aerosol loading is not constant on decadal time scales. For example, Mishchenko et al. (2007) show a globally decreasing trend in aerosol optical depth (AOD) over oceans beginning in the 1990s using observations from the Advanced Very High Resolution Radiometer (AVHRR), whereas Zhang and Reid (2010) report a statistically negligible positive global AOD trend over ocean from 2000 to 2009 using Moderate-Resolution Imaging Spectroradiometer (MODIS) and Multiangle Imaging Spectroradiometer (MISR) observations. In agreement with MODIS and MISR, a weakly positive trend in global AOD over ocean from 1998 to 2010 is also reported from Sea-viewing Wide Field-of-view Sensor (SeaWiFS) observations (Hsu et al. 2012). Differences in sensor calibration, cloud screening, assumptions of aerosol properties, and surface influences all impact the retrieval of AOD from satellite (Li et al. 2009). Erroneous retrievals of AOD may cause spurious trends that may mask the true magnitude of real aerosol trends (e.g., Mishchenko et al. 2012; Zhao et al. 2013).

The natural spatiotemporal variability of aerosols further complicates global assessments of AOD (e.g., Kaufman et al. 2002; Remer et al. 2008; Li et al. 2014). Because of subtleties in both magnitude and sign that are seen globally, the reconciliation of discrepancies hinges on regional analyses. Stronger regional trends are anticipated that should be easier to detect and quantify relative to global trends (Mishchenko and Geogdzhayev 2007). For example, trends from studies using AVHRR, MODIS, and SeaWiFS agree with a positive trend over Southeast Asia while regions of Europe and the United States exhibit negative trends (Zhao et al. 2008; Hsu et al. 2012; Zhang and Reid 2010). The increase in aerosol over Southeast Asia has been associated with rapid economic growth and the use of ''dirty'' energy, while decreases in aerosol over Europe are associated with clean-air legislations and the dissolution of the former Soviet Union. Decreases seen over North America are consistent with decreases in industrial emissions as a result of enactment of similar clean-air legislation (Mishchenko and Geogdzhayev 2007; Zhao et al. 2008; Hsu et al. 2012). Additional analysis using surface-based Aerosol Robotic Network (AERONET) observations adds confirmation to these regional satellite-observed trends in total AOD (e.g., de Meij et al. 2012; Li et al. 2014), but limited insight has been gained regarding the causes of the trends.

Changes in the mean aerosol loading over time can come from changes in precursor emissions of both natural and anthropogenic origins, as well as changes in meteorology. Natural changes in aerosol loading such as dust can be caused by changes in wind speed as well as surface wetness over arid regions (Mishchenko and Geogdzhayev 2007; Chin et al. 2014). Wind speed additionally influences marine aerosol loading (Smirnov et al. 2003). Anthropogenic changes in aerosol loading arise largely from changes in emissions driven by policy decision and socioeconomic factors. In the United States, the Environmental Protection Agency (EPA) sets and updates the National Ambient Air Quality Standards (NAAQS) for pollutants that are hazardous to both public health and the environment—standards that have continued to become more strict since inception in the 1970s with the Clean Air Act (U.S. EPA 2004a,b). Over the Southeast United States, individual studies have identified both correlation (Engel-Cox et al. 2004) as well as decreasing trends (Alston et al. 2012) in surface $PM_{2.5}$ and satellite AOD and implicate regulations as being successful in decreasing precursor emissions, $PM_{2.5}$ concentrations, and AOD (Gan et al. 2014). The strong correlations between $PM_{2.5}$ and AOD seen over the eastern United States may be due in part to relatively uniform aerosol type, height, and loadings compared to other areas where mismatches between surface-observed and satellite-assumed aerosol properties and plume heights may lead to poorer comparisons (Engel-Cox et al. 2004; Hoff and Christopher 2009). Additional factors that may weaken $PM_{2.5}$–AOD correlation include hygroscopic growth under high relative humidity and scenes with particle size distributions that include significant coarse-mode aerosol mass (Green et al. 2009). Yet, Wang and Christopher (2003) have shown that $PM_{2.5}$ and AOD correlations improve when monthly mean data are considered, as is in the present study. Changes in emissions and AOD can alter cloud properties via ACIs and further affect both radiative budget and regional climate individually and in combination. Changes in AOD have been shown to alter both surface and top-of-atmosphere radiation budgets (solar dimming/brightening) and have been suggested as a masker of the true impact of rising greenhouse gas concentrations and global warming (Li 1998; Wild et al. 2007). Caution and forethought when addressing air quality and climate must be properly exercised and due diligence performed. Poorly crafted policies to addressing short-lived forcers can have potentially large and regionally impactful consequences through unforeseen pathways like ACI (Shindell et al. 2012; Fischer-Bruns et al. 2010; Koren et al. 2007).

In this work, we explore changes in atmospheric aerosol loading over the eastern seaboard of the United States and the North Atlantic Ocean during the period from 2002 to 2012. We analyze trends in satellite and

surface AOD observations. By combining additional surface-based observations and aerosol model output, we are able to attribute some significant AOD trends as the results of trends in natural or anthropogenic aerosol species. Using satellite, ground, and model data allows for the attribution more reliably than any single source can suggest where the strengths of one data type can augment the deficiencies of others. This work expands on previous studies by considering the anthropogenic effects downwind of any significant anthropogenic sources.

This paper is presented as follows. Section 2 describes the data products employed for this work. Section 3 contains results of AOD trend analysis from satellite and surface observational datasets. Section 4 discusses the attribution of AOD trends as resulting from predominately natural or anthropogenic species. Section 5 discusses some of the limitations and uncertainties in the present study. Finally, section 6 summarizes this study.

2. Datasets

We employ three observational and two model datasets. Observations from NASA's MODIS satellite sensor, NASA's AERONET, and the EPA's Interagency Monitoring of Protected Visual Environments (IMPROVE) surface networks are used together with model results from NASA's Goddard Chemistry Aerosol Radiation and Transport (GOCART) and Modern-Era Retrospective Analysis for Research and Application (MERRA) models.

a. MODIS Level-3 monthly dataset

The MODIS sensor is a key instrument in NASA's Earth Observing System (EOS) mission and studies the entire earth system. MODIS consists of 36 spectral bands spanning wavelengths from 0.41 to 14.24 μm and has a spatial resolution of 0.25, 0.5, or 1.0 km depending on band. MODIS observations from the reflective solar bands (0.41 to 2.2 μm) are calibrated on board once in orbit and provide stability, accuracy, and degradation monitoring (Xiong et al. 2010). Accurate radiance observations are especially needed in long-term aerosol studies. Sensors that lack onboard calibration capabilities (like AVHRR) will show degradation in their radiometric signal that, if left uncorrected, can substantially influence both the calculation and significance of aerosol trends (Heidinger et al. 2010; Zhao et al. 2008).

For this work the MODIS Atmosphere Level-3 monthly mean product (MxD08_M3; Hubanks et al. 2015) with a 1° × 1° global spatial resolution from both Collection 051 and 006 are employed. Specifically, analysis using the AOD at 550 nm is explored using data from NASA's MODIS sensors on board *Aqua*. The AOD is obtained from the Level-2 aerosol product (MxD04_L2) and is derived from precomputed radiative transfer lookup tables (LUTs) at seven wavelengths between 0.47 and 2.12 μm. Over ocean, the "best" AOD is taken as the weighted combinations of four fine and five coarse modes that minimize the fitting errors between the observed and appropriate LUT reflectances, and the MODIS L2 aerosol products are in agreement with AERONET retrievals and are within their retrieval uncertainty [(0.03 ± 0.05)AOD] over oceans (Remer et al. 2008). Initially, Level-2 aerosol product retrievals at 10-km resolution are gridded to 1° × 1° resolution using a simple unweighted mean to create the Level-3 daily mean product. A further simple, unweighted mean of the Level-3 daily product produces the Level-3 monthly mean product (Hubanks et al. 2015). Data from MODIS *Aqua* are used, beginning in July 2002 and ending in December 2012. The upgrade from Collection 051 to 006 was aimed at "maintenance and modest improvement" and does not represent a major upgrade to algorithms or products (Levy et al. 2013). Quality assurance products are also available and the results of trend analysis using this dataset will also be discussed. Unless otherwise noted, the nominal MODIS AOD monthly Level-3 product from Collection 006 is used.

b. GSFC and CPVD AERONET sites

AERONET is a ground-based global network of sun photometers providing high-quality automatic observations of spectral AOD at a high frequency (Holben et al. 1998). AERONET has a proven record of being used as ground truth to validate numerous satellite AOD products from a variety of sensors (e.g., Zhao et al. 2004), including MODIS (Levy et al. 2010; Mi et al. 2007). In this work, we utilize the AERONET sites at Goddard Space Flight Center (GSFC) located in Greenbelt, Maryland (38.992°N, 76.840°W); Maryland Science Center (MDSC) located in Baltimore, Maryland (39.283°N, 76.617°W); and City College of New York (CCNY) in New York, New York (40.821°N, 73.949°W). We use the monthly mean AOD at 500 nm from the Level 2.0 product using the Version 2 direct sun algorithm (Holben et al. 2006) during the time period July 2002 to December 2012. The locations of the GSFC and CCNY AERONET sites used for correlation analysis in this work are shown in Fig. 1.

c. IMPROVE network

The IMPROVE network was established in 1988 and consists of ground-based long-term aerosol and particulate matter speciation observations at more than 150

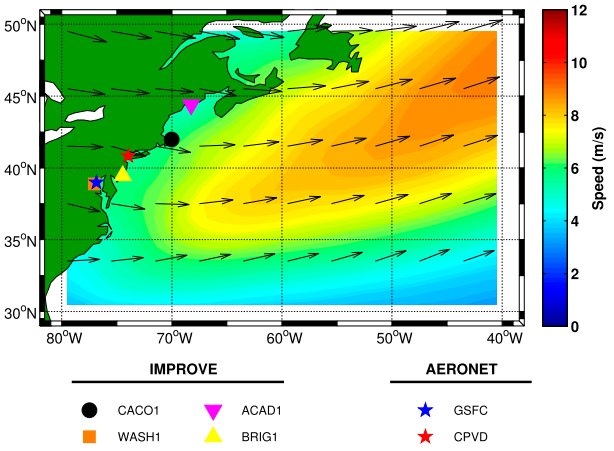

FIG. 1. The North Atlantic Ocean domain and climatological circulation at 850 hPa averaged during July 2002 to December 2012. Color contouring is for wind speed and arrows are wind direction. Locations of the IMPROVE and AERONET sites used in this study are also shown.

national wilderness and park locations across the United States. In 1999, the U.S. EPA, in collaboration with federal and state air and land managers, announced the Regional Haze Program (RHP) to improve air quality and visibility conditions in the nation's Class I areas (visually protected federal areas; http://www.epa.gov/visibility/visibility-regional-haze-program). The IMPROVE Network collects 24-h air samples every third day, and IMPROVE data have been used to monitor the absolute mass concentration, relative contribution, and seasonality of various species of $PM_{2.5}$ (Malm et al. 1994; Hand et al. 2011). For this study, we have obtained IMPROVE data from the "IMPROVE Aerosol, RHR (New Equation)" dataset (code: IMPRHR2; http://views.cira.colostate.edu/fed/DataWizard/Default.aspx) at four sites in the eastern United States and examine six species: ammonium sulfate (AS), ammonium nitrate (AN), particulate organic matter (POM), light-absorbing carbon (LAC), soil (SOIL), and sea salt (SS) and their sum total (TOT). We construct a simple monthly mean mass observation for each of the species and their combined total during 2002 to 2012. The four sites considered in the domain of this work include Washington, D.C. (WASH1; 38.876°N, 77.034°W); Cape Cod, Massachusetts (CACO1; 41.976°N, 70.024°W); Arcadia, Maine (ACAD1; 44.337°N, 68.261°W); and Brigantine, New Jersey (BRIG1; 39.465°N, 74.449°W). Their locations are shown in Fig. 1.

d. GOCART aerosol model

The GOCART model is a global chemical transport model that simulates tropospheric aerosol components throughout their lifetime, including emission, chemistry, advection, boundary layer mixing, moist convection, and wet and dry deposition (Chin et al. 2002). GOCART uses reanalysis meteorology from the Modern-Era Retrospective Analysis for Research and Applications (MERRA), and it is configured at a horizontal resolution of 0.50° latitude by 1.25° longitude with 72 vertical levels (Chin et al. 2014). The time step for advection, convection, and diffusion processes is 20 min and 60 min for other processes (Chin et al. 2000).

Anthropogenic emissions for the GOCART simulation used in this study are taken from the A2-ACCMIP and A2-MAP emissions datasets [Chin et al. (2014), Diehl et al. (2012), and references therein]. Monthly fossil fuel emissions are interpolated from RCP8.5 projections for years 2000, 2005, and 2010. Ten land-based anthropogenic sectors are interpolated to constant yearly emissions while those from international shipping are interpolated using the Emissions Database for Global Atmospheric Research 32FT2000 dataset for year 2000. Monthly emissions from aircraft are interpolated from a base year of 1992 with projections for use in 2015. Biomass burning emissions for the A2-ACCMIP dataset are derived from the Global Fire Emissions Database (GFED), version 2. These emissions are used because of their broad acceptance by modelers as well as their long coverage during the past decades (Chin et al. 2014).

Natural emissions for GOCART are parameterized using various methods. Land-based organic carbon emissions are parameterized from foliar density and biome-dependent emissions factor and are sensitive to photosynthetically active radiation and leaf temperature (Guenther et al. 1995). Emissions of dimethyl sulfide (DMS) from the ocean are parameterized from DMS concentration, water viscosity, and the 10-m wind (Lana et al. 2011), while sea salt emission is also parameterized from the 10-m wind (Chin et al. 2002). Daily volcanic emissions of SO_2 are used from the Smithsonian Institution's Global Volcanism Program (http://www.volcano.si.edu/). Finally, desert dust is parameterized from surface bareness, elevation, wetness, and 10-m wind (Ginoux et al. 2001).

GOCART computes AOD for each species based on column mass concentration and assumed optical, density, and size properties [see Chin et al. (2002)]. GOCART outputs the instantaneous spectral column AOD every 3 h for species include sulfate (SU), dust (DU), organic carbon (OC), black carbon (BC), sea salt (SS), and total (TOT) components of the AOD (Chin et al. 2014). For this work, monthly mean column AOD at 550 nm are calculated for each species and the total for the period from 2001 to 2009.

e. MERRA atmospheric reanalysis

MERRA is an atmospheric reanalysis product generated using NASA's Goddard Earth Observing System

(GEOS) atmospheric model (v5.2.0; GEOS-5) and data assimilation system (DAS). It is designed to more accurately represent the hydrological cycle by assimilation of winds, rain, and radiance data from a wide array of surface and satellite sources (including MODIS) as well as international soundings (Rienecker et al. 2011). MERRA produces 3-hourly output at a horizontal resolution of 0.50° latitude by 0.66° longitude on 72 vertical levels along with products at various spatiotemporal scales. Monthly mean horizontal winds (u and v) at 850 hPa (~1.5 km) are used presently to show the lower atmosphere climatological circulation.

3. Analyses and results

a. Methods of analysis

The geographical region selected for this work is the North Atlantic oceanic region (30°–50°N, 80°–40°W). This region is selected because oceanic AOD retrievals from space suffer smaller uncertainties than land (Levy et al. 2009) and the region is downwind of major continental sources of aerosol as shown in Fig. 1. Two overlapping time periods are examined: July 2002 through December 2012 covering data from MODIS *Aqua* and January 2001 through December 2009 covering data from the high-resolution GOCART aerosol model. Each of the datasets passes through a three-step analysis consisting of 1) deseasonalization, 2) linear regression, and 3) application of significance testing (the Student's t test). The goal is to analyze the interannual behavior of any observed trends, and, as such, the mean seasonal climatology is first removed (i.e., deseasonalized) following Eq. (1) below:

$$\tau_d(m,y) = \tau_n(m,y) - \tau_c(m), \tag{1}$$

where $\tau_n(m, y)$ is the native AOD time series, $\tau_c(m)$ is the year-round monthly AOD climatology, $\tau_d(m, y)$ is the deseasonalized AOD time series, and m and y are the month and year, respectively.

A simple linear regression is used to calculate the least squares estimate of the trend (slope) of the deseasonalized time series, formulated as $Y = a + bX$, where X is time and Y is the estimated value from a linear regression with offset a and slope b. The statistical significance of this calculated trend is found using a Student's t test and Eq. (2a) below, where b is the slope, σ is the standard deviation, and $S = \sum(X_i - \overline{X})^2$ (von Storch and Zwiers 1999). The statistical significance of an aerosol component trend is tested against the respective total so as to focus on component trends that are significant in the context of the total. Correlation analysis between two deseasonalized datasets is also performed and the significance is similarly tested using Eq. (2b) below, where R is the correlation coefficient and n is the degrees of freedom (i.e., number of months):

$$T = \frac{b}{\sigma/\sqrt{S}} \quad \text{and} \tag{2a}$$

$$T = |R|\sqrt{\frac{n-1}{1-R^2}}. \tag{2b}$$

The levels of significance are computed for both the 90% and 95% confidence intervals using a null hypothesis $H_0 = 0$ to compare both the computed trends to a series with no trend (i.e., H_0: $b = 0$) and the computed correlation against two series with no correlation (i.e., H_0: $R = 0$). The formulation of Eqs. (2a) and (2b) above reflect the null hypothesis H_0, and values for both t scores are dependent on the degrees of freedom of a time series (i.e., number of months) and are compared against a table for the Student's t distribution (von Storch and Zwiers 1999).

Finally, seasonal trends are computed for some datasets using a deseasonalized monthly record. The seasons are divided into December, January, and February (DJF; winter); March, April, and May (MAM; spring); June, July, and August (JJA; summer); and September, October, and November (SON; fall). Seasonal time series are first generated using the mean of deseasonalized observations within each of the seasons and year (December is used with the following year's January and February). A simple linear regression calculates the least squares estimate of the trend (slope) of the seasonal time series and statistical significance tested using Eq. (2a).

b. Observation-based AOD trends

1) MODIS

Persistent climatological circulations seen in MERRA (see Fig. 1) tend to transport aerosols in an expected manner. Aerosols emitted from North America are advected eastward to the North Atlantic Ocean in the midlatitudes; therefore, at least part of AOD changes over the region may be traced to changes in the emissions over the upwind continent. Deseasonalized trends in the total AOD observed from MODIS identify a distinct region over the North Atlantic Ocean. Figure 2 shows the existence of a significant (marked by crosses) negative AOD trend in the midlatitudes. This negative AOD trend has a magnitude around −0.020 to −0.040 decade^{-1}, is statistically significant above the 95% level [calculated from Eq. (2a)], and is spatially expansive and coherent. A comparison of trends from Collection 051 (Fig. 2a) and Collection 006 (Fig. 2b) reveals similarity in the existence

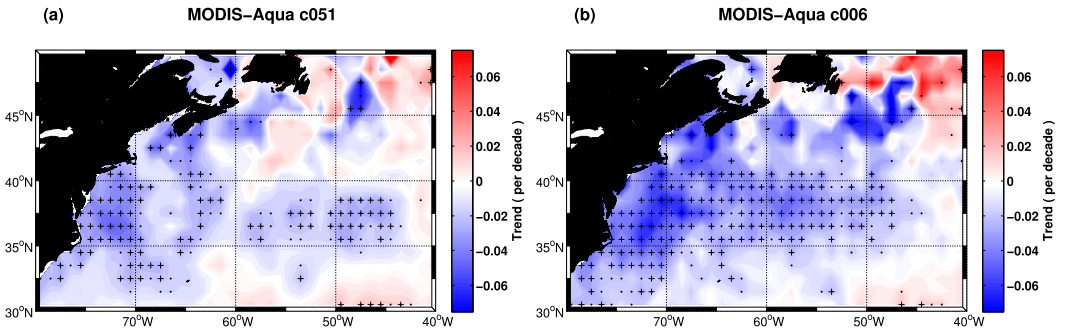

FIG. 2. Deseasonalized AOD trends from MODIS *Aqua* over the North Atlantic Ocean during July 2002 to December 2012 for (a) Collection 051 and (b) Collection 006. Dots and plus signs represent statistically significant trends at the 90% and 95% levels, respectively. AOD trends are per decade.

of a negative trend in the midlatitudes who share similar magnitudes and significance across the two products. The midlatitude trend found in this study shows general agreement with the values of $-0.015\,\text{decade}^{-1}$ reported by Zhang and Reid (2010) with MODIS from 2000 to 2009 and $-0.04\,\text{decade}^{-1}$ reported by Hsu et al. (2012) with SeaWiFS from 1998 to 2010 in the eastern North American–North Atlantic region. This is also in agreement with a -0.02-decade^{-1} trend for a different period reported by Zhao et al. (2008) with AVHRR from 1985 to 2005.

2) AERONET

To explore if the trends in AOD over the ocean originate from changes in the upwind continental region, trends in deseasonalized AOD from three AERONET sites along the eastern United States are calculated. These three sites are used under the consideration that they may represent aerosol loading and species typically predominant in the source regions upwind of the North Atlantic Ocean [e.g., anthropogenic aerosols (such as sulfates) in the midlatitudes]. Figure 3 shows the deseasonalized monthly mean AOD and linear fit from 2002 to 2012 for the three AERONET sites. There is a negative trend ranging between -0.07 and $-0.08\,\text{decade}^{-1}$ at the GSFC, MDSC, and CCNY sites (significant at the 95% level), which suggests decreasing aerosol loading over the eastern United States. The trend at GSFC agrees with those found previously (e.g., Hsu et al. 2012). The usage and agreement between these sites signifies the decreasing AOD trend is not just local but exists on a regional scale along the eastern United States.

3) CORRELATIONS BETWEEN MODIS AND AERONET

To understand the spatial variability of AOD and the connection between satellite retrievals over the large domain with ground observations at fixed sites, a spatial correlation between deseasonalized AOD from MODIS over the North Atlantic Ocean and the GSFC and CCNY AERONET sites is computed. Correlations with the MDSC site are not included as they are similar to those from GSFC. The results from correlations with MODIS monthly AOD during the period July 2002 to December 2012 are shown in Fig. 4. The correlation analysis identifies a region of the total aerosol field in the midlatitudes downwind of the U.S. coast that has a strong correlation (>0.6) with both the GSFC and CCNY sites, with minimal correlations elsewhere. This region also exhibits correlations significant at the 95% level using Eq. (2b). Intuitively, these results suggest that the behavior and trends in the total aerosol loading (see Fig. 2) occurring in the region are a consequence of changes in the emission and transport of the predominant aerosol species from the upwind region. Strong correlations with GSFC (Fig. 4, left) and CCNY (Fig. 4, right) suggest anthropogenic changes from North America. The results also point to the role of large-scale circulation (shown in Fig. 1) over the North Atlantic blowing from west to east in the midlatitudes. When considered in totality (Figs. 1–4), the region appears to be under influence of large-scale circulation patterns that transport aerosol species from upwind sources and that share similar trends from surface and satellite observation.

4. Attribution of the trends: Contributions of natural or anthropogenic aerosols

a. GOCART AOD trends

To further examine the relative role of individual aerosol species in the total AOD observed by MODIS, trends of five aerosol species simulated by GOCART are calculated. Employing output from an aerosol model can complement the capability of MODIS by providing

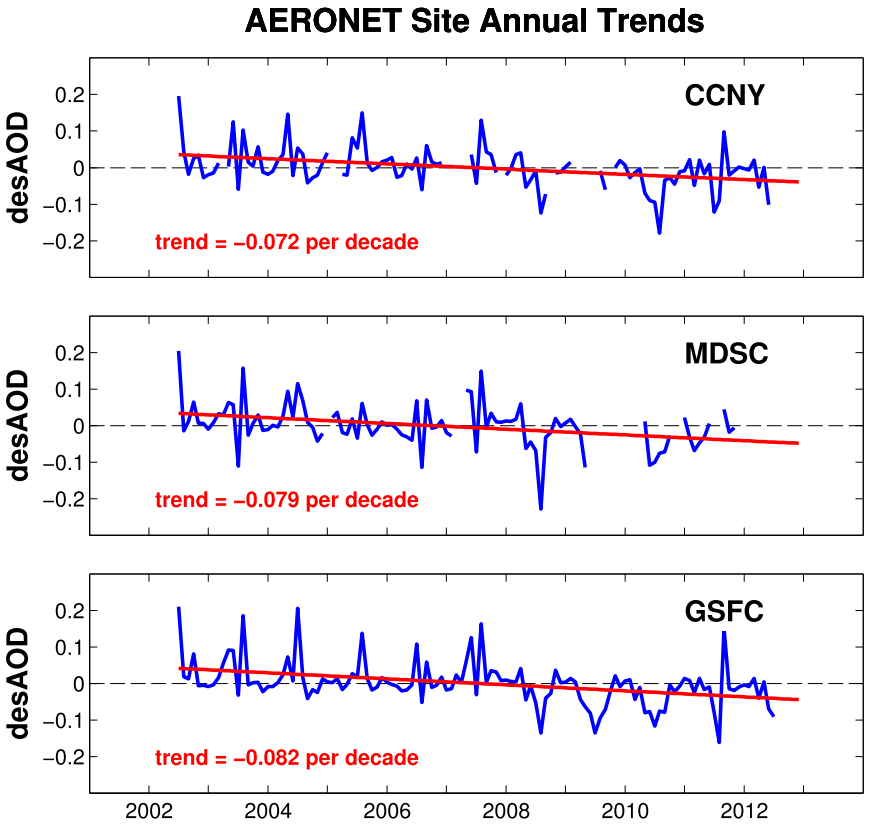

FIG. 3. Deseasonalized AOD records from July 2002 to December 2012 for the three AERONET sites at 500 nm. The thick red line represents a statistically significant linear trend reported in the figure.

the constituent species composing the total loading. Trends in the total (TOT) AOD from GOCART are first compared to those observed from MODIS in the total AOD before examining any species. Figure 5a shows the deseasonalized trend in the TOT AOD over the North Atlantic Ocean as seen in GOCART during January 2001 to December 2009. When compared to the AOD trends observed from MODIS (Fig. 2), the trend from GOCART show similarity. There exists a negative trend (around $-0.015\,\text{decade}^{-1}$) in the GOCART TOT AOD within the domain. This trend is roughly collocated with that from MODIS observations and is found to be statistically significant using Eq. (2a).

An assessment of trends in the five individual species aids in revealing the species responsible for the trends in the AOD from MODIS. In addition to trends in the total AOD, Fig. 5 also shows the deseasonalized trends for the predominately natural (DU + SS; Fig. 5b) and

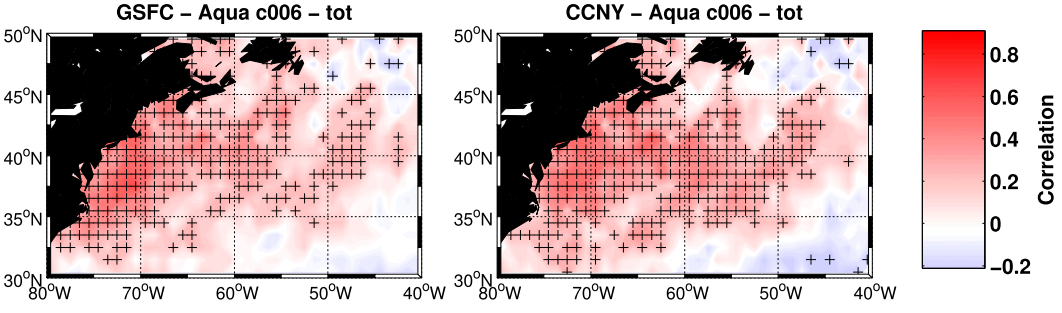

FIG. 4. Spatial distribution of deseasonalized AOD temporal correlation of MODIS *Aqua* with (left) GSFC and (right) CCNY over the North Atlantic Ocean during July 2002 to December 2012. Plus symbols represent statistically significant correlations at the 95% level.

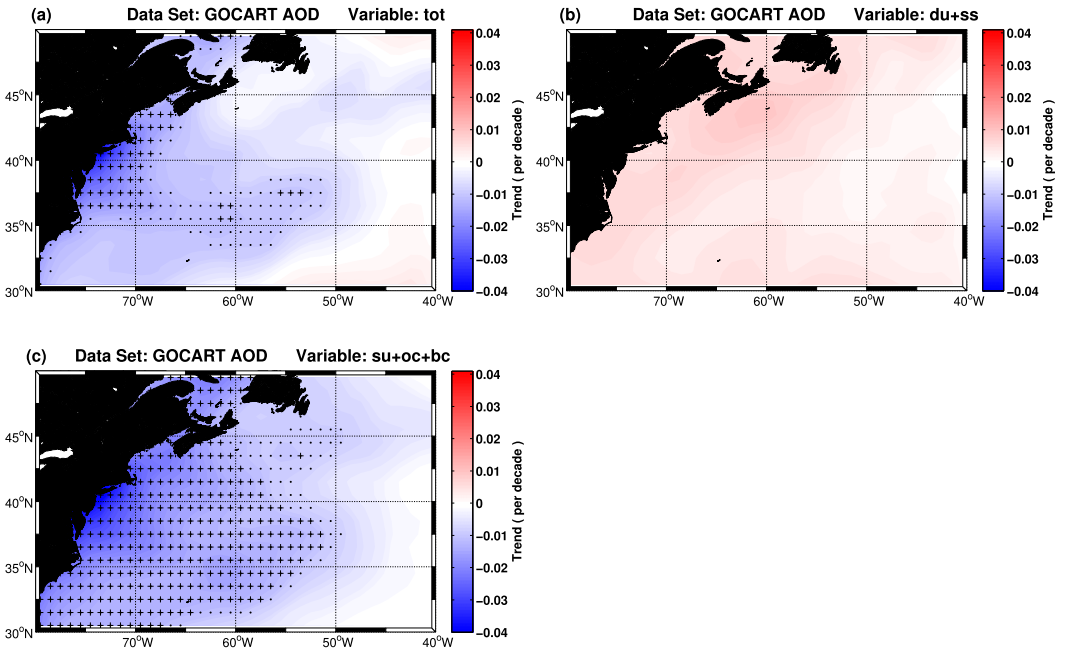

FIG. 5. Deseasonalized AOD trends from GOCART for the North Atlantic Ocean during January 2001 to December 2009. Dots and plus symbols represent trends significant at the 90% and 95% levels, respectively. All trends are per decade: (a) total (TOT), (b) natural (SS + DU), and (c) anthropogenic (SU + OC + BC).

anthropogenic (SU + BC + OC; Fig. 5c) components. Readily observable is a strong and significant negative trend (around $-0.020\,\text{decade}^{-1}$) in the anthropogenic AOD components. This trend is located in the western midlatitudes off the coast of North America and is collocated well with the negative trends in the total AOD suggested by GOCART and observed by MODIS. GOCART thus provides strong evidence for the region being under the influence of a predominately anthropogenic change in aerosol loading. Trends for all five aerosol species individually are shown in appendix A.

b. *IMPROVE network $PM_{2.5}$ species trends*

Trends in surface aerosol $PM_{2.5}$ species observed at four IMPROVE locations provide additional information on the anthropogenic origin of negative AOD trend in the midlatitudes observed by MODIS and calculated from GOCART. Figure 6 presents the native, relative contribution, and deseasonalized monthly mean $PM_{2.5}$ time series for the Washington, D.C. IMPROVE site during July 2002 to December 2012. As can be seen, AS is the dominate contributor (upward of 60% and twice that of any other species) to the total $PM_{2.5}$ throughout the summertime, while AS, AN, and POM contribute relatively equally during wintertime. An analysis of the deseasonalized data reveals that the TOT particulate mass experiences a $-7.726\,\mu\text{g}\,\text{m}^{-3}\,\text{decade}^{-1}$ trend. Componentwise, the Washington, D.C., site experiences a $-4.278\,\mu\text{g}\,\text{m}^{-3}\,\text{decade}^{-1}$ trend in AS and a $-1.867\,\mu\text{g}\,\text{m}^{-3}\,\text{decade}^{-1}$ trend in POM.

Extending this analysis to the other three IMPROVE sites further reinforces the finding that anthropogenic species are the main driver of the negative AOD trend seen from MODIS and in GOCART. Figure 7 shows the calculated $PM_{2.5}$ decadal trends from all four IMPROVE sites (see Fig. 1 for locations) during July 2002 to December 2012. All sites report significant decreasing trends in total $PM_{2.5}$, and all sites report significant decreases in ammonium sulfate mass. A significant trend in POM is flagged at the Washington, D.C. (WASH1), site. This POM trend may be reflective of recent controls on anthropogenic volatile organic carbon (VOC) emissions, an important precursor of POM. No other species report a statistically significant trend at any of the sites.

c. *Observed seasonal trends*

As seen in Fig. 7, significant decreases in AS appear to be the main driver of the total $PM_{2.5}$ decreases at the IMPROVE sites considered. Sulfate aerosols from SO_2 typically peak during summertime (Hidy et al. 1978) and have been shown to account for in excess of 50% of surface $PM_{2.5}$ over the eastern United States [e.g., Fig. 6; see also Hand et al. (2012)]. Thus, we investigate any seasonal trends that exist in our observational datasets and if they offer further support to the anthropogenic origin of the decreases in AOD.

Figure 8 shows the seasonal trends in deseasonalized AOD trends from MODIS. The trends in SON and DJF seasons are relatively weak when compared to the

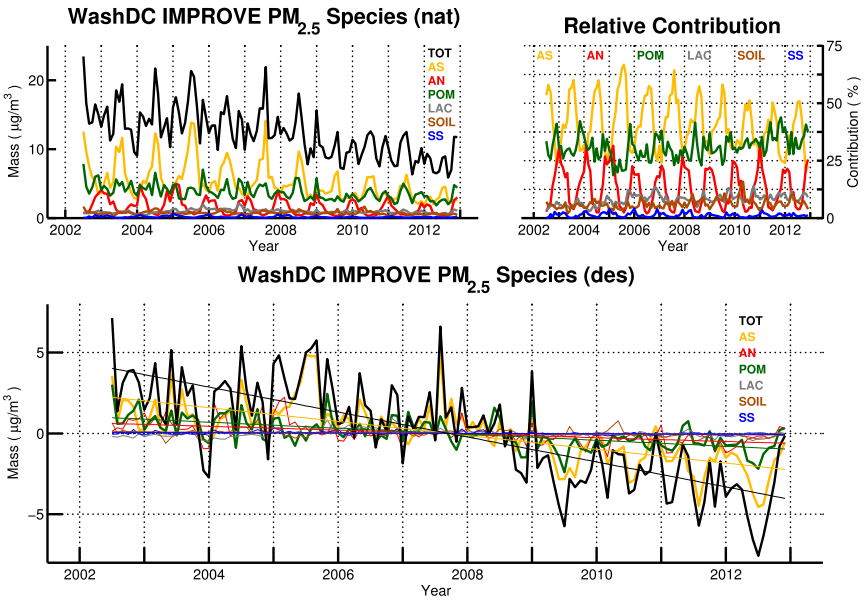

FIG. 6. $PM_{2.5}$ records from the Washington, D.C., IMPROVE site (38.88°N, 77.03°W) during July 2002 to December 2012 for ammonium sulfate (AS; yellow), ammonium nitrate (AN; red), particulate organic matter (POM; green), light-absorbing carbon (LAC; gray), SOIL (brown), sea salt (SS; blue), and total (TOT; black) species. Shown are the (top left) native, (top right) relative contribution, and (bottom) deseasonalized time series. Superimposed on the deseasonalized time series are the calculated linear regression lines. Only those that are significant beyond the 95% level are in bold (AS, POM, and TOT).

strong decreasing trends seen in MAM and JJA. An assessment of AERONET site seasonal trends reveals a similar pattern. Figure 9 displays the seasonal breakdown of deseasonalized AOD at the GSFC, MDSC, and CCNY AERONET sites. The trends are not significant during SON or DJF seasons at any of the sites. GSFC reports a -0.07-decade^{-1} trend in MAM. The CCNY and MDSC sites also suggest a decreasing trend during MAM—however, neither being significant at the 95% significance level. At both CCNY and GSFC, the decreasing trends are significant during JJA: -0.195 and -0.233 decade^{-1}, respectively. At the MDSC site, the decrease seems rather strong in JJA but it is not statistically significant owing to too large of variance and/or too few data points [see Eq. (2a)].

Having considered the optical aerosol load from both satellite (MODIS) and surface (AERONET), seasonal trends in the aerosol surface $PM_{2.5}$ species are now examined. Figure 10 (top) shows the seasonal trends in deseasonalized total $PM_{2.5}$ mass observed at each of the four IMPROVE surface network sites. While significant trends may be seen in any of the four seasons across the sites considered, the strongest trends are seen to occur during the MAM and JJA seasons. The smallest trends are seen in the SON and DJF seasons, some of which are not statistically significant. These four sites along the Northeast coast reveal notable decreases specifically during the JJA season when compared to other seasons—trends that are upward of twice as large as other seasons. Seasonal trends are computed for the six PM species considered from the IMPROVE sites. It is determined that AS is the only species to demonstrate statistically significant trends when compared to the total PM behavior for a given site and season (Fig. 10, bottom). Importantly, strong statistically significant decreases in AS are seen most notably during the JJA season and also to a lesser extent during the MAM season when considering these four northeastern IMPROVE sites.

To further the highlight the spring and summer decreases, consider the annual AERONET and Washington, D.C., IMPROVE site (WASH1) along with the seasonal IMPROVE trends. From the AERONET sites (Fig. 3), substantial negative deseasonalized AOD values can be seen during the summertime months at each site beginning around 2008. When considering the $PM_{2.5}$ behavior at the WASH1 (Fig. 6), summertime reductions in TOT and AS species can be seen also beginning around 2008. These months coincide with the large fractional make up that AS contributes to the total $PM_{2.5}$ load. We believe this timing to identify the beginning of control measures in the Northeast and mid-Atlantic

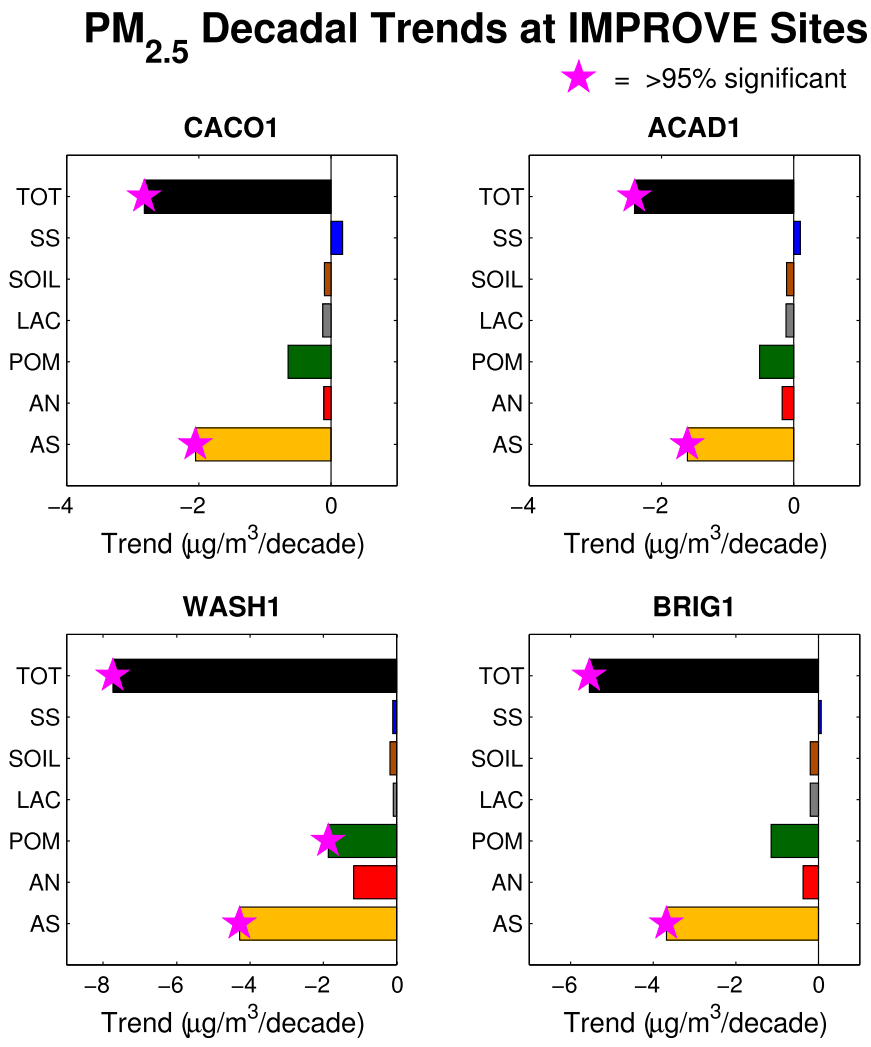

FIG. 7. $PM_{2.5}$ decadal trends from the four IMPROVE sites (see Fig. 1 for locations) during July 2002 to December 2012 for ammonium sulfate (AS; yellow), ammonium nitrate (AN; red), particulate organic matter (POM; green), light-absorbing carbon (LAC; gray), SOIL (brown), sea salt (SS; blue), and total (TOT; black) species. Statistical significance at the 95% level is denoted by the pink stars. Note the different scales used. Trend units are in $\mu m\, m^{-3}$ decade^{-1}.

regions to meet air-quality standards set out in the EPA's 2005 Clean Air Interstate Rule and subsequently replaced with the Cross-State Air Pollution Rule in 2011 (https://www.epa.gov/crossstaterule/).

5. Discussion

While the analyses of the extensive datasets provide compelling evidence and causes of the various trends, it is necessary to note some of the potential limitations and uncertainties that may undermine some of the findings. Uncertainties in the trend, correlation, and significance calculations can arise from a large standard deviation of the deseasonalized time series as well as the length (number of observations; alternatively degrees of freedom) under consideration [see Eq. (2)]. Autocorrelation between observations can degrade the ability to detect a trend and/or reduce the significance calculated. To mitigate this impact, we avoid the uncertainties associated with autocorrelation by removing the seasonal cycle (deseasonalizing) and then computing the trends on the deseasonalized anomalies.

Additionally, there may also be factors within the retrieval algorithm that lead to uncertainties in the observed MODIS AOD. These may include the effects of aerosol "swelling" (a function of relative humidity), three-dimensional cloud effects, potential mismatches in cloud masking, and method of aggregation (Levy

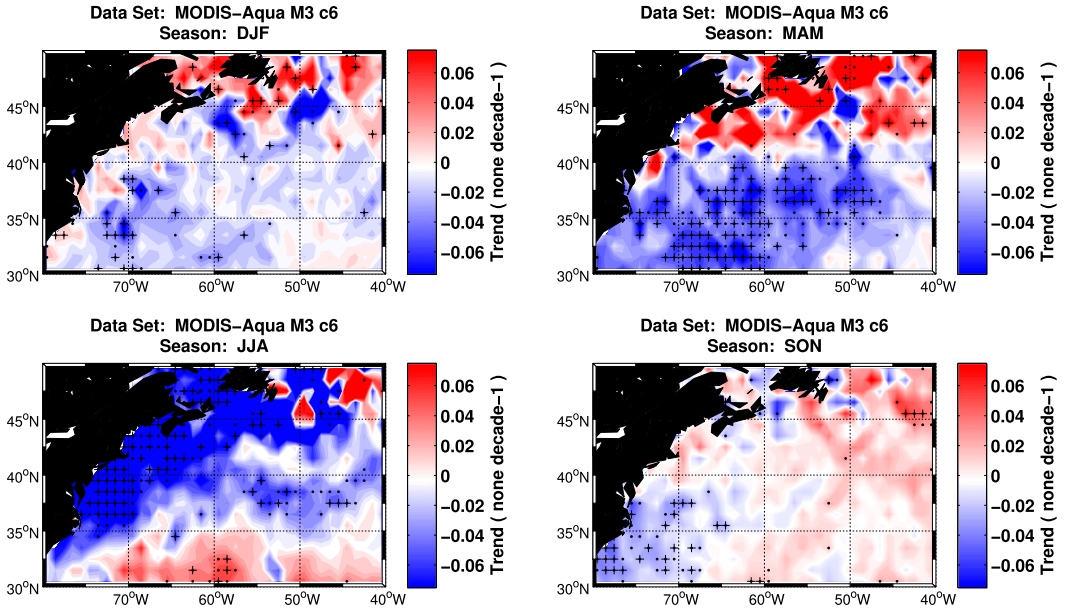

FIG. 8. Seasonal trends of deseasonalized AOD from MODIS *Aqua* over the North Atlantic Ocean during July 2002 to December 2012 for Collection 6. Dots and plus symbols represent statistically significant trends at the 90% and 95% levels, respectively. AOD trends are per decade.

et al. 2009, 2013; Li et al. 2009). These factors may affect the initial AOD retrieval and subsequently cascade into calculation of the AOD trend. Yet, the large-scale similarity in AOD trends from MODIS *Aqua* between Collection 051 and 006 (Fig. 2) seen in this study adds faith to both the radiometric stability of the sensor as well as the accurate assessment of aerosol performed by the retrieval algorithm (and improvements) in the context of the monthly mean data used here. The most notable difference between the two collections is the stronger decrease and more extensive significance of the midlatitude trend seen in Collection 6. We believe this to be caused in part by changes to upstream inputs prior to the aerosol retrieval—notably, changes in radiance calibration, gas correction, cloud masking, and a modified wind speed dependence of the surface over ocean (Levy et al. 2013). These changes largely cause AOD from Collection 6 to be lower than that of Collection 5. One postretrieval change that was made to the Level-3 monthly products is the removal of pixel weighting. Aerosol retrievals are already clear-sky biased, and the pixel weighting proved to further this bias (Levy et al. 2013). The removal of pixel weighting has the result of increasing AOD in Collection 6 relative to Collection 5. While outside the scope of the present study, we believe that the improvements in cloud masking and removal of pixel weighting to play an important role in the differences, especially for a region that experiences periodic storminess. Finally, the MODIS Level-3 product also contains a ''quality assurance'' or QA product, in which the Level-2 AOD retrievals are weighted by their quality flag (QA = 0–3, 3 being best) based on numerous criteria during the retrieval algorithm (Levy et al. 2013). Trends in the deseasonalized QA AOD from MODIS *Aqua* Collection 6 during July 2002 to December 2012 are displayed in Fig. 11. There exists exceptional similarity in AOD trends when using the QA product (Fig. 11) and the nominal AOD product (Fig. 2b), and trends in all regions appear faithful regardless of product (QA or nominal) chosen.

Uncertainties in the GOCART aerosol dataset may arise from several sources, including inaccurate emission inputs and improper parameterizations within the GOCART model. Using aerosol loading results from chemical transport models must be taken cautiously and limitations understood, as AOD uncertainties relative to AERONET can be large (e.g., Chin et al. 2002) and significant variance in AOD may exist across model estimates (e.g., Myhre et al. 2013; Kim et al. 2014). Using the projections of anthropogenic emissions (RCP8.5) in the A2-ACCMIP dataset may induce uncertainty as emissions during 2001 to 2009 are interpolated from yearly projection values for 2000, 2005, and 2010. Linear interpolation may further eliminate real or impose artificial seasonality on emissions pattern for individual species. Yet when compared to emissions inventories for the United States, the A2-ACCMIP anthropogenic emissions showed small differences, likely due to

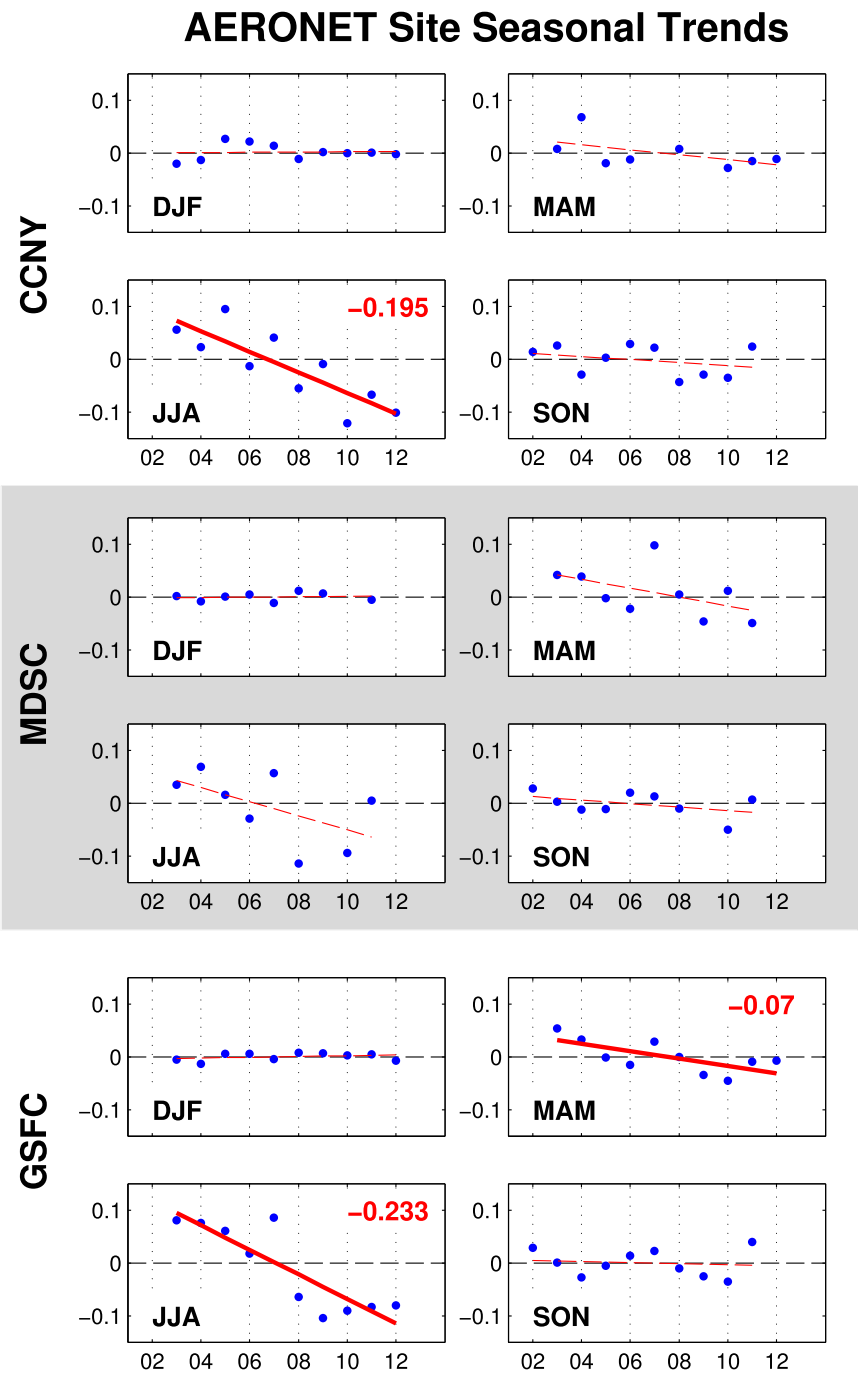

FIG. 9. Seasonal trends of deseasonalized AOD from AERONET sites in the eastern United States during July 2002 to December 2012. Thick red lines represent statistically significant trends at the 95% level. Significant AOD trends reported in the figure are per decade.

accurate reporting of activity and continuous measurements (Chin et al. 2014; Diehl et al. 2012). Additionally, dust in GOCART may be overestimated while biomass burning may be underestimated (Chin et al. 2014). Another potential source of discrepancy between MODIS and GOCART AODs arises from the use of slightly different aerosol physical properties assumed and approach to get AOD: MODIS generates radiance lookup tables for aerosol inversion while GOCART uses a mass to optical extinction conversion (Chin et al. 2002; Levy et al. 2009). Finally, a comparison between IMPROVE data and GOCART model runs over the United States

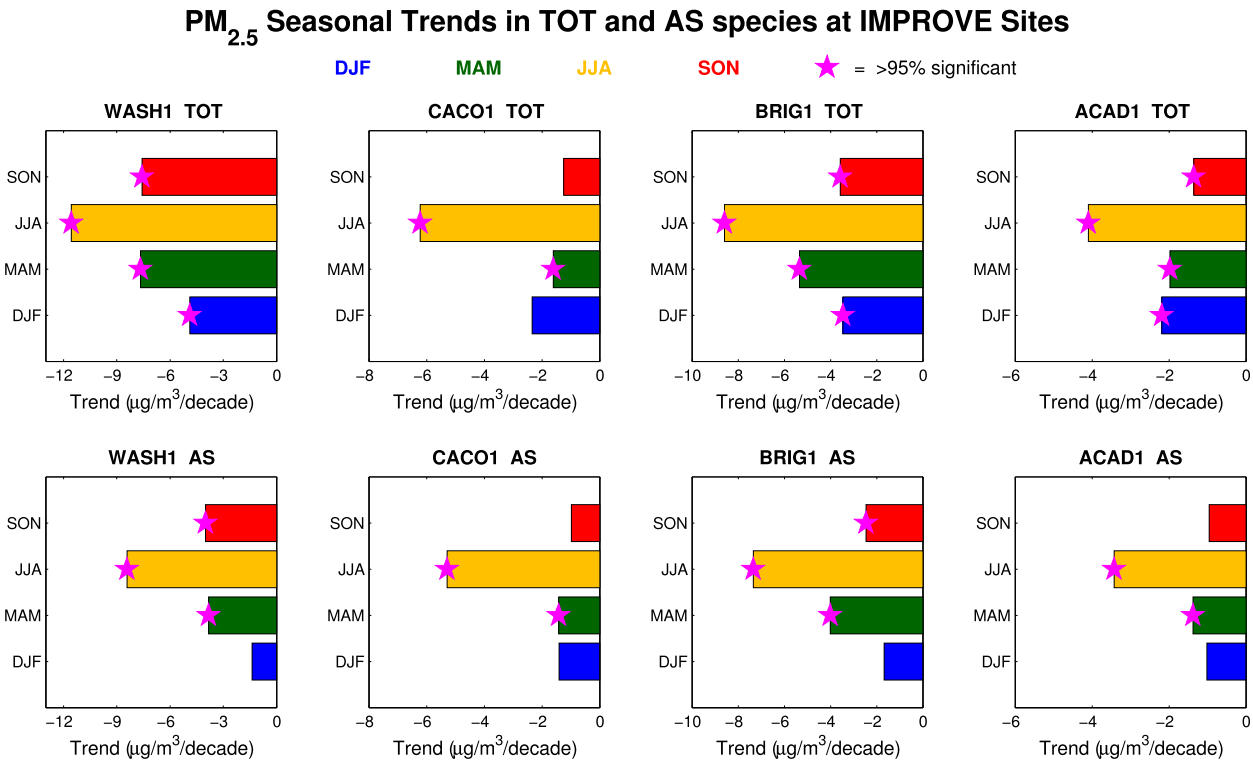

FIG. 10. Seasonal trends in $PM_{2.5}$ from the four IMPROVE sites (see Fig. 1 for locations) during July 2002 to December 2012 for (top) total (TOT) species and (bottom) ammonium sulfate (AS) species only. Statistical significance at the 95% level is denoted by the pink stars. Trend units are in $\mu m\, m^{-3}$ decade^{-1}.

show good correlation between reconstructed fine mass as well as sulfate; however, slightly weaker correlations are shown for fine dust and nonbiomass carbonaceous species (Chin et al. 2007). The importance of local U.S. emissions of aerosol species relative to long-range transport and strong correlations between local emissions, surface concentrations, and AOD have been demonstrated between GOCART and IMPROVE (Chin et al. 2007; 2014).

We presently note some clarification for the correlation analysis performed between AERONET and MODIS AOD. AERONET is commonly used as a reference to compare satellite-retrieved AOD to, including MODIS (e.g., Levy et al. 2009, 2010, 2013). These validation studies compare Level-2 granule MODIS data with AERONET, typically in a 50 km× 50 km area surrounding the AERONET site and within 30 min of MODIS overpass. Here, we do not aim to validate the accuracy of MODIS monthly AOD against AERONET. We are primarily concerned with the degree of shared variability between MODIS and AERONET and not a comparison of absolute AOD value. We simply present a spatial extent of the correlation strength between monthly deseasonalized AOD from AERONET and MODIS.

6. Conclusions

Aerosols contribute both directly and indirectly to atmospheric variability and to the earth's radiative balance; however, their impacts remain uncertain. Because of their natural spatiotemporal variability, studies assessing global aerosol trends offer conflicting results while regional studies begin to show more consistency

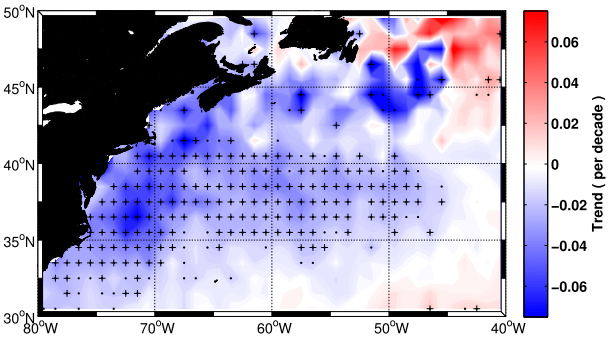

FIG. 11. Deseasonalized AOD trends using the QA AOD product from MODIS *Aqua* over the North Atlantic Ocean during July 2002 to December 2012 for Collection 6. Dots and plus signs represent statistically significant trends at the 90% and 95% levels, respectively. AOD trends are per decade.

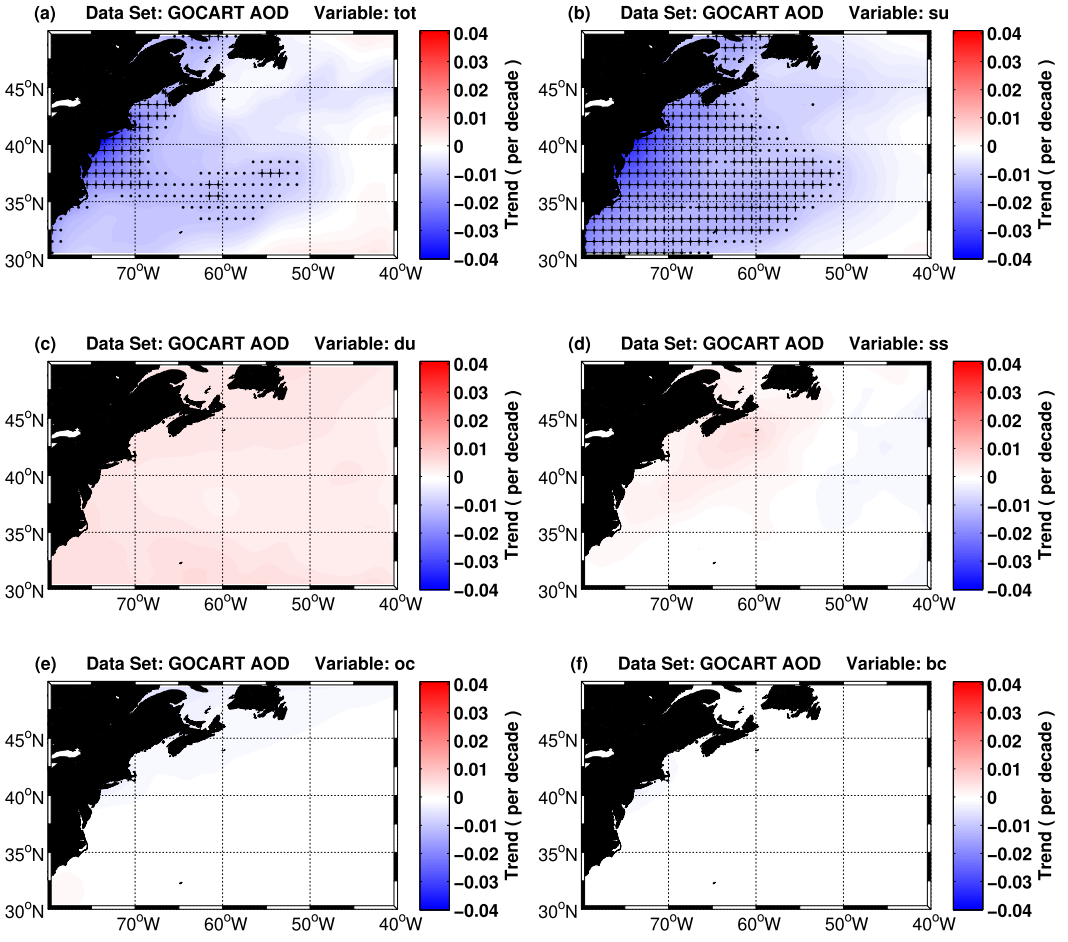

FIG. A1. Deseasonalized AOD trends from GOCART for the North Atlantic during January 2001 to December 2009. Dots and plus signs represent trends significant at the 90% and 95% levels, respectively. All trends are per decade. (a) Total (TOT), (b) sulfate (SU), (c) dust (DU), (d) sea salt (SS), (e) organic carbon (OC), and (f) black carbon (BC).

across sensors, which, by themselves, provide very little insight into the causes. Changes to the atmospheric aerosol loading can arise from changes in source location and strength, chemical evolution, and transport. To untangle the contributions of these factors to any observed trends requires the combined use of satellite and surface observations with model simulations.

This study takes advantage of combining datasets from satellite (MODIS), surface (AERONET and IMPROVE), and model (GOCART and MERRA) to investigate trends in aerosol loading (via AOD) and their causes over the North Atlantic Ocean from 2002 to 2012. Robust, statistically significant negative AOD trends are found in the midlatitudes. Analysis of AERONET stations (at GSFC, MDSC, and CCNY sites) in the upwind source region reveals decreasing AOD over the eastern United States while correlation analysis between MODIS and GSFC and CCNY AERONET sites reveals strong downwind correlation over the North Atlantic and suggests that changes in the total AOD are the consequence of changes in the (predominantly anthropogenic) aerosol species in the region.

To further understand the causes of the trends, GOCART model simulations of five aerosol component species are used. The trend of the total AOD shows similar magnitude, significance, and extent as those observed from MODIS. The sums of predominately anthropogenic (SU + OC+ BC) versus natural (SS + DU) species suggest that the strong aerosol trend is anthropogenic in the midlatitudes. This ''fingerprinting'' of the type of species is further strengthened by analyses of $PM_{2.5}$ observations at four IMPROVE sites in the eastern United States. Significant negative annual trends are found for ammonium sulfate at all IMPROVE sites, organic matter at only one site, and no other trends for any other sites and/or species. Determination of seasonal trends reveals strong decreases in AOD from both MODIS and AERONET during spring and summer.

Analysis of seasonal IMPROVE $PM_{2.5}$ observations show strong decreases during these months, which correspond to strong and significant decreases in ammonium sulfate.

The findings of this study offer additional insight into the success of EPA regulations in air-quality control, whose main aim was to reduce levels of air pollutants including $PM_{2.5}$. Not only have these regulations seen decreases in AOD over the source regions, but as shown here also resulted in a reduction of AOD beyond the source regions of air pollutants. A reduction in aerosol loading is expected to bring about changes in clouds over the North Atlantic via complex aerosol–cloud interactions. Impacts may range from altering the direct radiation received at the surface to modifying precipitation intensity/location, cloud morphology, and ultimately the TOA radiation budget. Further studies are warranted to investigate these impacts of changing aerosol loading on clouds and radiation from a climate perspective, both in the North Atlantic region as well as others around the world that may also exhibit long-term trends in aerosol loading.

Acknowledgments. The authors would like to acknowledge Dr. Rob Levy of the MODIS Aerosol Team for valuable discussions as well as Dr. Mian Chin for providing access to the high-resolution GOCART simulation used presently. MERRA atmospheric reanalysis data were acquired from NASA's Goddard Earth Sciences (GES) Data and Information Services Center (DISC). We also thank the Principal Investigators of the AERONET network for maintaining and allowing access to their data. Finally, IMPROVE is a collaborative association of state, tribal, and federal agencies and international partners. The U.S. EPA is the primary funding source, with contracting and research support from the National Park Service. The Air Quality Group at the University of California, Davis, is the central analytical laboratory, with ion analysis provided by Research Triangle Institute, and carbon analysis provided by Desert Research Institute. The authors also thank two anonymous reviewers for their helpful comments. This research is supported by the grants of NSF (AGS1534670), NSFC (91544217), and MOST (2013CB955804).

APPENDIX

GOCART Species Trends

Shown in Fig. A1 is the trend and significance analysis applied to all individual GOCART species. Apparent is the lack of strong and significant trends over the North Atlantic for dust, sea salt, organic carbon, and black carbon. It is thus sensible to combine the components into predominately natural (dust and sea salt) and anthropogenic (sulfate, black carbon, organic carbon) components.

REFERENCES

Alston, E. J., I. N. Sokolik, and O. V. Kalashnikova, 2012: Characterization of atmospheric aerosol in the US Southeast from ground- and space-based measurements over the past decade. *Atmos. Meas. Tech.*, **5**, 1667–1682, doi:10.5194/amt-5-1667-2012.

Chin, M., R. B. Rood, S.-J. Lin, J.-F. Muller, and A. M. Thompson, 2000: Atmospheric sulfur cycle simulated in the global model GOCART: Model description and global properties. *J. Geophys. Res.*, **105**, 24 671–24 687, doi:10.1029/2000JD900384.

——, and Coauthors, 2002: Tropospheric aerosol optical thickness from the GOCART model and comparisons with satellite and sun photometer measurements. *J. Atmos. Sci.*, **59**, 461–483, doi:10.1175/1520-0469(2002)059<0461:TAOTFT>2.0.CO;2.

——, T. Diehl, P. Ginoux, and W. Malm, 2007: Intercontinental transport of pollution and dust aerosols: Implications for regional air quality. *Atmos. Chem. Phys.*, **7**, 5501–5517, doi:10.5194/acp-7-5501-2007.

——, and Coauthors, 2014: Multi-decadal aerosol variations from 1980 to 2009: A perspective from observations and a global model. *Atmos. Chem. Phys.*, **14**, 3657–3690, doi:10.5194/acp-14-3657-2014.

de Meij, A., A. Pozzer, and J. Lelieveld, 2012: Trend analysis in aerosol optical depths and pollutant emission estimates between 2000 and 2009. *Atmos. Environ.*, **51**, 75–85, doi:10.1016/j.atmosenv.2012.01.059.

Diehl, T., A. Heil, M. Chin, X. Pan, D. Streets, M. Schultz, and S. Kinne, 2012: Anthropogenic, biomass burning, and volcanic emissions of black carbon, organic carbon, and SO_2 from 1980 to 2010 for hindcast model experiments. *Atmos. Chem. Phys. Discuss.*, **12**, 24 895–24 954, doi:10.5194/acpd-12-24895-2012.

Engel-Cox, J. A., C. H. Hollman, B. W. Coutant, and R. M. Hoff, 2004: Qualitative and quantitative evaluation of MODIS satellite sensor data for regional and urban scale air quality. *Atmos. Environ.*, **38**, 2495–2509, doi:10.1016/j.atmosenv.2004.01.039.

Fischer-Bruns, I., J. Feichter, S. Kloster, and A. Schneidereit, 2010: How present aerosol pollution from North America impacts North Atlantic climate. *Tellus*, **62A**, 579–589, doi:10.1111/j.1600-0870.2010.00446.x.

Gan, C.-M., J. Pleim, R. Mathur, C. Hogrefe, C. N. Long, J. Xing, S. Rossel, and C. Wei, 2014: Assessment of the effect of air pollution controls on trends in shortwave radiation over the United States from 1995 through 2010 from multiple observation networks. *Atmos. Chem. Phys.*, **14**, 1701–1715, doi:10.5194/acp-14-1701-2014.

Ginoux, P., M. Chin, I. Tegen, J. M. Prospero, B. Holben, O. Dubovik, and S.-J. Lin, 2001: Sources and distributions of dust aerosols simulated with the GOCART model. *J. Geophys. Res.*, **106**, 20 255–20 273, doi:10.1029/2000JD000053.

Green, M., S. Kondragunta, P. Clren, and C. Xu, 2009: Comparison of GOES and MODIS Aerosol Optical Depth (AOD) to Aerosol Robotic Network (AERONET) AOD and IMPROVE $PM_{2.5}$ mass at Bondville, Illinois. *J. Air Waste Manage. Assoc.*, **59**, 1082–1091, doi:10.3155/1047-3289.59.9.1082.

Guenther, A., and Coauthors, 1995: A global model of natural volatile organic compound emissions. *J. Geophys. Res.*, **100**, 8873–8892, doi:10.1029/94JD02950.

Hand, J. L., and Coauthors, 2011: IMPROVE (Interagency Monitoring of Protected Visual Environments): Spatial and seasonal patterns and temporal variability of haze and its constituents in the United States. Cooperative Institute for Research in the Atmosphere Rep. V, 507 pp. [Available online at http://vista.cira.colostate.edu/Improve/spatial-and-seasonal-patterns-and-temporal-variability-of-haze-and-its-constituents-in-the-united-states-report-v-june-2011/.]

——, B. A. Schichtel, M. Pitchford, W. C. Malm, and N. H. Frand, 2012: Seasonal composition of remote and urban fine particulate matter in the United States. *J. Geophys. Res.*, **117**, D05209, doi:10.1029/2011JD017122.

Heidinger, A. K., W. C. Straka III, C. C. Molling, J. T. Sullivan, and X. Wu, 2010: Deriving an inter-sensor consistent calibration for the AVHRR solar reflectance data record. *Int. J. Remote Sens.*, **31**, 6493–6517, doi:10.1080/01431161.2010.496472.

Hidy, G. M., P. K. Mueller, and E. Y. Tong, 1978: Spatial and temporal distributions of airborne sulfate in parts of the United States. *Atmos. Environ.*, **12**, 735–752, doi:10.1016/0004-6981(78)90255-X.

Hoff, R. M., and S. A. Christopher, 2009: Remote sensing of particulate pollution from space: Have we reached the promised land? *J. Air Waste Manag. Assoc.*, **59**, 646–675.

Holben, B. N., and Coauthors, 1998: AERONET—A federated instrument network and data archive for aerosol characterization. *Remote Sens. Environ.*, **66**, 1–16, doi:10.1016/S0034-4257(98)00031-5.

——, R. F. Eck, I. Slutsker, A. Smirnov, A. Sinyuk, J. Schafer, D. Giles, and O. Dubovik, 2006: AERONET's Version 2.0 quality assurance criteria. *Remote Sensing of the Atmosphere and Clouds*, S.-C. Tsay et al., Eds., International Society for Optical Engineering (SPIE Proceedings, Vol. 6408), 64080Q, doi:10.1117/12.706524.

Hsu, N. C., R. Gautam, A. M. Sayer, C. Bettenhausen, C. Li, M. J. Jeong, S.-C. Tsay, and B. N. Holben, 2012: Global and regional trends of aerosol optical depth over land and ocean using SeaWiFS measurements from 1997 to 2010. *Atmos. Chem. Phys.*, **12**, 8037–8053, doi:10.5194/acp-12-8037-2012.

Hubanks, P., S. Platnick, M. King, and B. Ridgway, 2015: MODIS Atmosphere L3 gridded product algorithm theoretical basis document (ATBD) & users guide. MODIS Algorithm Theoretical Basis Doc. ATBD-MOD-30, 119 pp. [Available online at http://modis-atmos.gsfc.nasa.gov/MOD08_M3/atbd.html.]

IPCC, 2013: *Climate Change 2013: The Physical Science Basis*. Cambridge University Press, 1535 pp., doi:10.1017/CBO9781107415324.

Kaufman, Y. J., D. Tanre, and O. Boucher, 2002: A satellite view of aerosols in the climate system. *Nature*, **419**, 215–223, doi:10.1038/nature01091.

Kim, D., and Coauthors, 2014: Sources, sinks, and transatlantic transport of North African dust aerosol: A multimodel analysis and comparison with remote sensing data. *J. Geophys. Res. Atmos.*, **119**, 6259–6277, doi:10.1002/2013JD021099.

Koren, I., L. A. Remer, and K. Longo, 2007: Reversal of trend of biomass burning in the Amazon. *Geophys. Res. Lett.*, **34**, L20404, doi:10.1029/2007GL031530.

Lana, A., and Coauthors, 2011: An updated climatology of surface dimethlysulfide concentrations and emission fluxes in the global ocean. *Global Biogeochem. Cycles*, **25**, GB1004, doi:10.1029/2010GB003850.

Levy, R. C., L. A. Remer, D. Tanré, S. Mattoo, and Y. J. Kaufman, 2009: Algorithm for remote sensing of tropospheric aerosol over dark targets from MODIS: Collections 005 and 051: Revision 2. NASA Algorithm Theoretical Basis Doc., 96 pp. [Available online at http://modis-atmos.gsfc.nasa.gov/_docs/ATBD_MOD04_C005_rev2.pdf.]

——, ——, R. G. Kleidman, S. Mattoo, C. Ichoku, R. Kahn, and T. F. Eck, 2010: Global evaluation of the Collection 5 MODIS dark-target aerosol products over land. *Atmos. Chem. Phys.*, **10**, 10 399–10 420, doi:10.5194/acp-10-10399-2010.

——, S. Mattoo, L. A. Munchak, L. A. Remer, A. M. Sayer, F. Patadia, and N. C. Hsu, 2013: The Collection 6 MODIS aerosol products over land and ocean. *Atmos. Meas. Tech.*, **6**, 2989–3034, doi:10.5194/amt-6-2989-2013.

Li, J., B. E. Carlson, O. Dubovik, and A. A. Lacis, 2014: Recent trends in aerosol optical properties derived from AERONET measurements. *Atmos. Chem. Phys.*, **14**, 12 271–12 289, doi:10.5194/acp-14-12271-2014.

Li, Z., 1998: Influence of absorbing aerosols on the inference of solar surface radiation budget and cloud absorption. *J. Climate*, **11**, 5–17, doi:10.1175/1520-0442(1998)011<0005:IOAAOT>2.0.CO;2.

——, and Coauthors, 2009: Uncertainties in satellite remote sensing of aerosols and impact on monitoring its long-term trend: A review and perspective. *Ann. Geophys.*, **27**, 2755–2770, doi:10.5194/angeo-27-2755-2009.

Malm, W. C., J. F. Sisler, D. Huffman, R. A. Eldred, and T. A. Cahill, 1994: Spatial and seasonal trends in particle concentration and optical extinction in the United States. *J. Geophys. Res.*, **99**, 1347–1370, doi:10.1029/93JD02916.

Mi, W., Z. Li, X. Xia, B. Holben, R. Levy, F. Zhao, H. Chen, and M. Cribb, 2007: Evaluation of the Moderate Resolution Imaging Spectroradiometer aerosol products at two Aerosol Robotic Network stations in China. *J. Geophys. Res.*, **112**, D22S08, doi:10.1029/2007JD008474.

Mishchenko, M. I., and I. V. Geogdzhayev, 2007: Satellite remote sensing reveals regional tropospheric aerosol trends. *Opt. Express*, **15**, 7423–7438, doi:10.1364/OE.15.007423.

——, ——, W. B. Rossow, B. Carins, B. E. Carlson, A. A. Lacis, L. Liu, and L. D. Travis, 2007: Long-term satellite record reveals likely recent aerosol trend. *Science*, **315**, 1543, doi:10.1126/science.1136709.

——, L. Liu, I. V. Geogdzhayev, J. Li, B. E. Carlson, A. A. Lacis, B. Cairns, and L. D. Travis, 2012: Aerosol retrievals from channel-1 and -2 AVHRR radiances: Long-term trends updated and revisited. *J. Quant. Spectrosc. Radiat. Transfer*, **113**, 1974–1980, doi:10.1016/j.jqsrt.2012.05.006.

Myhre, G., and Coauthors, 2013: Radiative forcing of the direct aerosol effect from AeroCom Phase II simulations. *Atmos. Chem. Phys.*, **13**, 1853–1877, doi:10.5194/acp-13-1853-2013.

Remer, L. A., and Coauthors, 2008: Global aerosol climatology from the MODIS satellite sensors. *J. Geophys. Res.*, **113**, D14S07, doi:10.1029/2007JD009661.

Rienecker, M. M., and Coauthors, 2011: MERRA: NASA's Modern-Era Retrospective Analysis for Research and Applications. *J. Climate*, **24**, 3624–3648, doi:10.1175/JCLI-D-11-00015.1.

Shindell, D. T., A. Voulgarakis, G. Faluvegi, and G. Milly, 2012: Precipitation response to regional radiative forcing. *Atmos. Chem. Phys.*, **12**, 6969–6982, doi:10.5194/acp-12-6969-2012.

Smirnov, A., B. N. Holben, T. F. Eck, O. Dubovik, and I. Slutsker, 2003: Effect of wind speed on columnar aerosol optical properties at Midway Island. *J. Geophys. Res.*, **108**, 4802, doi:10.1029/2002JD002701.

U.S. EPA, 2004a: Air quality criteria for particulate matter. Vol. 1, U.S. Environmental Protection Agency Final Rep. EPA

600/P-99/002aF, 900 pp. [Available online at https://cfpub2.epa.gov/ncea/risk/recordisplay.cfm?deid=87903.]

——, 2004b: Air quality criteria for particulate matter. Vol. 2, U.S. Environmental Protection Agency Final Rep. EPA 600/P-99/002bF, 1148 pp. [Available online at https://cfpub2.epa.gov/ncea/risk/recordisplay.cfm?deid=87903.]

von Storch, H., and F. W. Zwiers, 1999: *Statistical Analysis in Climate Research*. Cambridge University Press, 496 pp., doi:10.1017/CBO9780511612336.

Wang, J., and S. A. Christopher, 2003: Intercomparison between satellite-derived aerosol optical thickness and $PM_{2.5}$ mass: Implications for air quality studies. *Geophys. Res. Lett.*, **30**, 2095, doi:10.1029/2003GL018174.

Wild, M., A. Ohmura, and K. Makowski, 2007: Impact of global dimming and brightening on global warming. *Geophys. Res. Lett.*, **34**, L04702, doi:10.1029/2006GL028031.

Xiong, X., J. Sun, X. Xie, W. L. Barnes, and V. V. Salomonson, 2010: On-orbit calibration and performance of Aqua MODIS reflective solar bands. *IEEE Trans. Geosci. Remote Sens.*, **48**, 535–546, doi:10.1109/TGRS.2009.2024307.

Zhang, J., and J. S. Reid, 2010: A decadal regional and global trend analysis of the aerosol optical depth using a data-assimilation grade over-water MODIS and Level 2 MISR aerosol products. *Atmos. Chem. Phys.*, **10**, 10 949–10 963, doi:10.5194/acp-10-10949-2010.

Zhao, T. X.-P., O. Dubovik, A. Smirnov, B. Holben, J. Sapper, C. Pietras, K. Voss, and R. Frouin, 2004: Regional evaluation of an Advanced Very High Resolution Radiometer (AVHRR) two-channel aerosol retrieval algorithm. *J. Geophys. Res.*, **109**, D02204, doi:10.1029/2003JD003817.

——, I. Laszlo, W. Guo, A. Heidinger, C. Cao, A. Jelenak, D. Tarpley, and J. Sullivan, 2008: Study of long-term trend in aerosol optical thickness observed from operational AVHRR satellite instrument. *J. Geophys. Res.*, **113**, D07201, doi:10.1029/2007JD009061.

——, P. K. Chan, and A. K. Heidinger, 2013: A global survey of the effect of cloud contamination on the aerosol optical thickness and its long-term trend derived from operational AVHRR satellite observations. *J. Geophys. Res. Atmos.*, **118**, 2849–2857, doi:10.1002/jgrd.50278.